Paper accepted for presentation at 2003 IEEE Bologna PowerTech Conference, June 23-26, Bologna, Italy

Interaction of the Secondary Arc with the Transmission System during Single-Phase Autoreclosure

M. Kizilcay, *Member, IEEE*, G. Bán, *Fellow Member, IEEE*, L. Prikler, *Member, IEEE*, and P. Handl, *non-member*

Abstract **– Secondary arcs can be modeled in a numerical transients program like ATP-EMTP. The dynamic behavior of the arc is represented as a time-varying resistance by solving a differential equation of arc conductance based on the energy balance in the arc column. The almost random variation of arc parameters influences significantly the arc performance during single-phase autoreclosure on transmission lines. Depending on the variation of arc parameters, certain effects of interaction with the transmission system are observed. In this relation, field tests on real overhead lines are extremely useful to verify numerical arc simulations and to understand the arcing phenomenon. Authors have participated in the past in several field tests performed on a 400 kV overhead line without shunt compensation and on 750 kV line with shunt compensation.**

Index Terms **– autoreclosure, arc, arcing fault, EMTP, primary arc, secondary arc, shunt reactor, transients, transmission line.**

I. Introduction

FAULTS on EHV/UHV overhead lines are in majority single-phase-to-ground arcing faults and are temporary in most cases. *Single-phase auto-reclosure* (SPAR) is an effective measure to eliminate arcing faults. The fault arc is classified according to the fault state regarding the fault current. *Primary arc* is effective after fault inception till single-phase tripping of the faulty phase. *Secondary arc* follows the primary arc after isolating the fault by single-phase tripping on a transmission line. It is sustained by the capacitive and inductive coupling to the sound phases. The secondary arc self-extinguishes usually, but its life-time may have a strong influence to the operation of the line: the longer the secondary arcing time, the higher the risk of unsuccessful reclosing. Lengthening the SPAR dead time is limited by dynamic stability constraints. This limit is usually less than 1.5 - 2 seconds for long EHV/UHV interconnections.

Whereas the primary arc shows generally a deterministic behavior as observed at field and laboratory arc tests [1], [2], the secondary arc has extremely random characteristics effected by the external conditions around the arc channel like ionized surrounding air, wind, thermal buoyancy and electro-dynamic force. In spite of this fact, a numerical arc model may be an useful tool to identify the main influencing factors and the interaction of the arc with the electric circuit, and to guess worst-case arcing time.

M. Kizilcay is with the Dept. of Elect. Eng. & Comp. Sci., Osnabrueck University of Applied Sciences, Germany (e-mail: kizilcay@fhos.de)

G. Bán is with the Dept of Electric Power Engineering, Budapest University of Technology and Economics (e-mail: ban@vmt.bme.hu)

L. Prikler is with the Dept of Electric Power Engineering, Budapest University of Technology and Economics (e-mail: l.prikler@ieee.org)

P. Handl is PhD student at the Budapest University of Technology and Economics (e-mail: handlp@vmt.bme.hu)

II. Model of the Fault Arc

The arc model used in this work is based on the energy balance of the arc column and describes an arc in air by a differential equation of the arc conductance g [2], [3]:

$$\frac{dg}{dt} = \frac{1}{\tau}(G - g) \tag{1}$$

where τ: is the arc time constant,
g: instantaneous arc conductance,
G: stationary arc conductance.

The stationary arc conductance is defined as:

$$G = \frac{|i_{arc}|}{u_{st}} \tag{2}$$

with

$$u_{st} = \left(u'_0 + r'_0 |i_{arc}|\right) \cdot l_{arc}(t) \tag{3}$$

where i_{arc}: instantaneous arc current,
u_{st}: stationary arc voltage,
l_{arc}: instantaneous arc length,
u'_0: characteristic arc voltage per length,
r'_0: characteristic arc resistance per length.

Equation (1) is a generalized arc equation that is suitable to represent an arc in an electric circuit by a two-pole. The parameters τ, u'_0 and r'_0 can be obtained from arc measurements. In case of secondary arc they vary significantly with arc length l_{arc}. The dependence of the arc time constant τ on l_{arc} can be defined by the relation

$$\tau = \tau_0 \cdot \left(\frac{l_{arc}}{l_0}\right)^{\alpha} \tag{4}$$

where τ_0: initial time constant,
l_0: initial arc length,
α: coefficient of negative value.

0-7803-7967-5/03/$17.00 ©2003 IEEE

Since the length variation of the secondary arc is highly dependent on external factors like wind, thermal buoyancy, it is difficult to consider these random effects accurately in the arc model. Nevertheless the above arc model may be used successfully to estimate the maximum arcing time as worst case or to understand the interaction of the secondary arc with the electrical circuit.

A. Arc Representation in EMTP-ATP

The arc as a nonlinear dynamic element is represented by the *Thevenin type*, Type-94 component in the ElectroMagnetic Transients Program EMTP-ATP [4]. The arc is described in MODELS language. In the Thevenin type component the electric arc as a two-pole sees the rest of the linear circuit as a Thevenin equivalent. Inputs are Thevenin voltage v_{th} and resistance r_{th} at the terminals. The arc model calculates the value of the resulting arc current i_{arc} at each time step. The interaction of the electric arc with the remaining circuit is shown in Fig. 1.

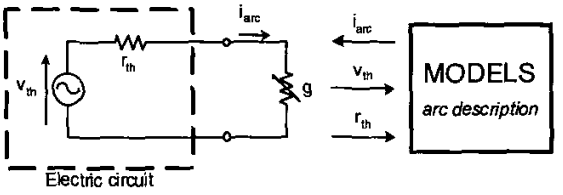

Fig. 1. Interaction between the electic circuit and the arc model

At each time step first the stationary arc voltage u_{st} and time constant τ are updated using (3) and (4) which depend on instantaneous arc length l_{arc}. The arc current i_{arc} can be expressed referring to Fig. 1 as follows

$$i_{arc} = \frac{g \cdot v_{th}}{1 + g \cdot r_{th}} \tag{5}$$

The arc equation (1) is solved using MODELS's LAPLACE function to obtain g:

$$g(t) = \frac{1}{1 + \tau \cdot s} \cdot G(t) \tag{6}$$

Equations (2), (5) and (6) are solved simultaneously using an iterative method available in MODELS as "COMBINE ITERATE ... ENDCOMBINE" [4]. The use of type-94 component in EMTP-ATP enables simultaneous solution of arc equations together with the equivalent system of the electric network.

B. Criteria for Self-Extinction of the Arc

The secondary arc elongation causes increase of arc voltage. If the arc elongation is rather smooth without steep rise, for example due to gust, then the secondary arc extinguishes as the arc voltage reaches the level of recovery voltage [5]. The recovery voltage is the voltage across the fault path at arc location after extinction of the secondary arc. Consequently, the arc duration may be estimated by the elongation speed of the arc.

Besides the arc elongation, re-ignitions inside the arc channel may have a significant role in the process. The speedy elongation of the arc separates the conducting plasma clouds by high resistance channel zones. So the resistance of the whole arc length increases. It often happens however, that the recovery voltage makes the high resistance arc channel zones re-ignite during the arc elongation process. If the recovery voltage is sufficient to produce a breakdown, bridging a significant length of the arc channel, the arcing process may return to the steady-state condition, remarkably prolonging the self-extinction time.

The arc self-extinction phenomenon is not known in detail. There are two different approaches that try to explain arc extinction: A) based on thermal instability described by arc equation (1). The arc extinguishes, if the time derivative of instantaneous arc resistance, dr_{arc}/dt, exceeds a pre-defined limit provided arc conductance g' per length is less than g'_{min}. B) based on dielectric phenomenon [6]. It is assumed that following each arc current reversal, the arc would first extinguish. The arc current is held at zero for as long as the arc recovery voltage remains below an arc re-ignition voltage characteristic obtained empirically.

C. Random Variation of Arc Parameters

Since the arc parameters are expressed as functions of the instantaneous arc length, the random arc behavior can be reproduced by varying the arc length in a random way. It is physically reasonable to describe a global arc length increase – either piecewise-linear or any predefined function – superposed by a local random length variations that should imitate the local breakdowns along the elongated secondary arc. Fig. 2 shows an example of arc length variation that is used to simulate fault arc whose voltage and current waveforms were recorded at a field test performed on a 230 km long, 400-kV overhead line without shunt compensation as shown in Fig. 3 [2]. The line has been operated by connecting the two circuits in parallel along the 1/3rd of the full length. The remaining sections of the 2nd circuit have been disconnected from the tested line or were grounded.

Fig. 4 and 5 show the measured and computed arc voltages and currents, respectively. The steady-state recovery voltage is shown additionally in Fig. 4. When the secondary arc voltage reaches the level of recovery voltage, the arc extinguishes. For the arc simulation following arc data are used:

$$u'_0 = 0.9\ \text{kV/m}, \quad \tau_0 = 1\ \text{ms}$$
$$r'_0 = 22\ \text{m}\Omega\text{/m}; \quad \alpha = -0.5.$$

Initial length of the primary arc is assumed as 4 m. For arc extinction the following limiting values per arc length were used:

$$g'_{\min} = 50\,\mu\text{S}\cdot\text{m},$$

$$\frac{dr'_{arc}}{dt} = 20\,\text{M}\Omega/(\text{s}\cdot\text{m})$$

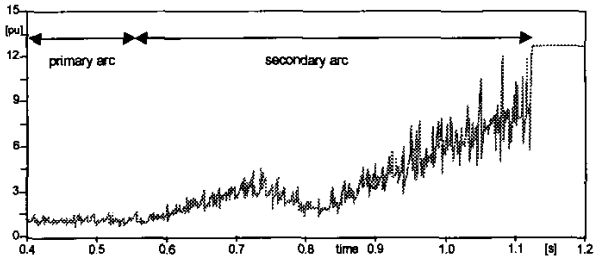

Fig. 2. Time-varying arc length with random local variations

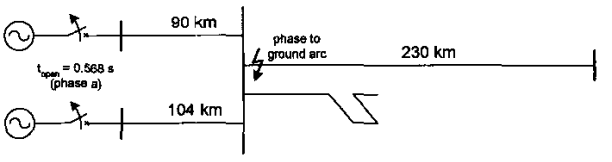

Fig. 3. 400-kV transmission system with arc tests

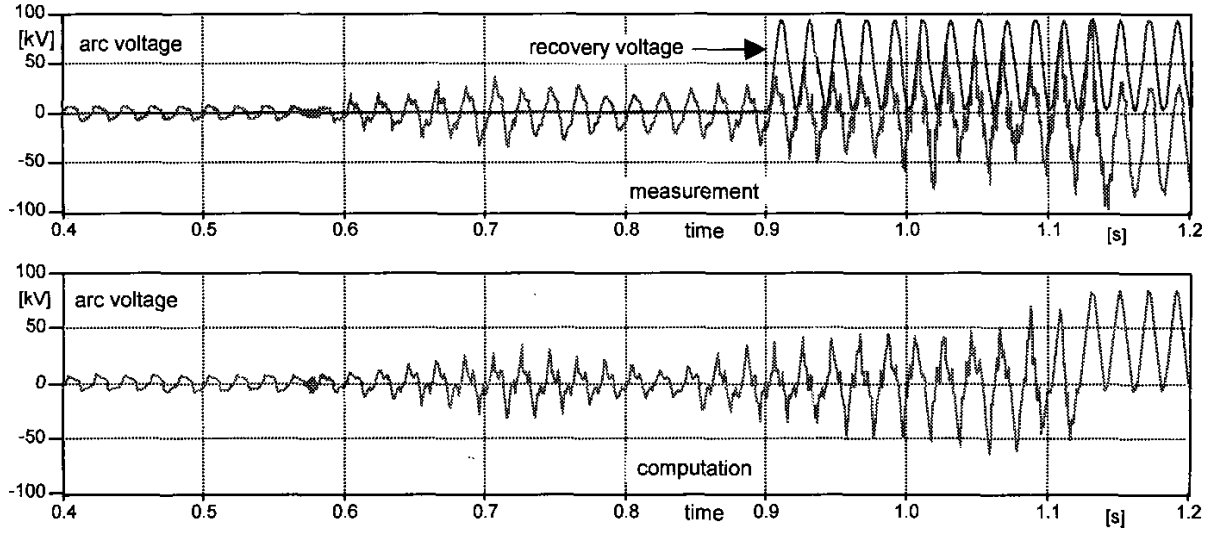

Fig. 4. Measured and computed arc voltages

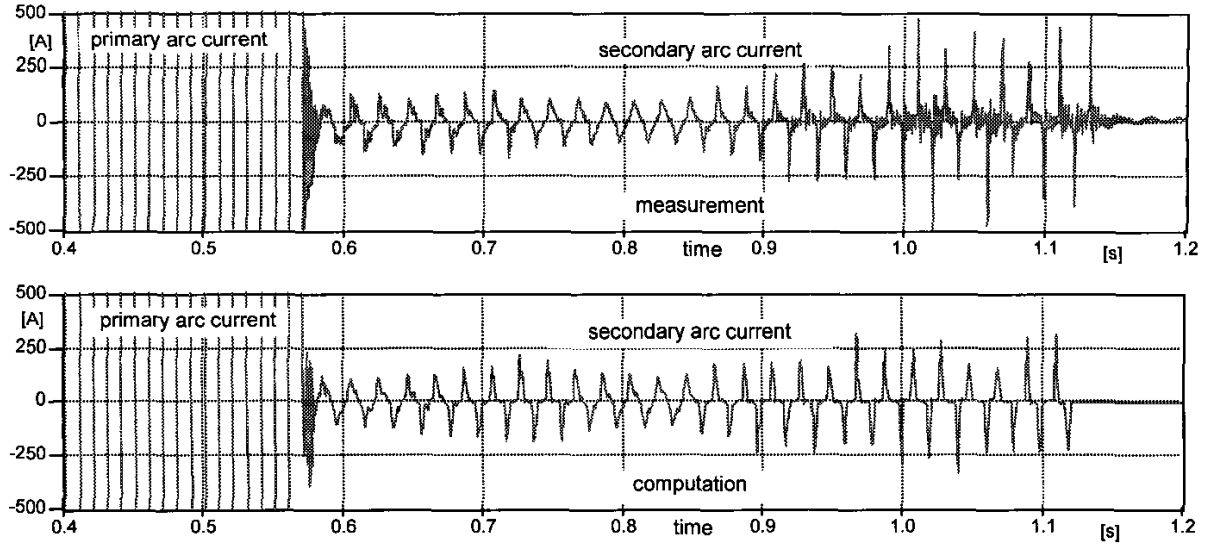

Fig. 5. Measured and computed arc currents

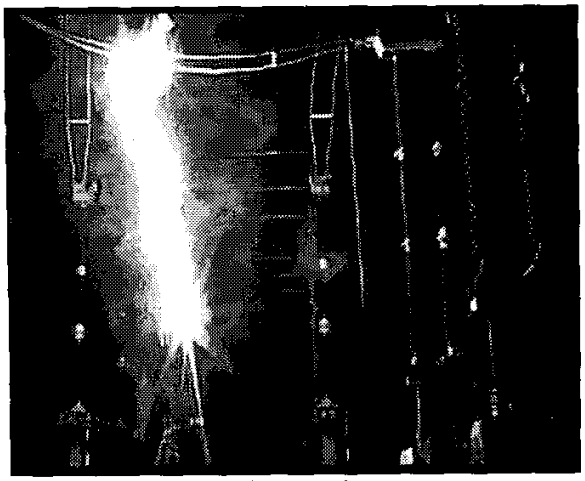

Fig. 6. Sustained 400-kV secondary arc at calmness

III. Excitation of Traveling Waves on the Line by the Secondary Arc

In the field tests of secondary arc performance on a double-circuit, 400-kV overhead line of 230 km length without shunt compensation the authors from Budapest identified from records of arcs (see Fig. 6) at calmness with long self-extinction times that the arc re-ignitions (transition from a very low arc conductance state to a high conductance state) initiate traveling waves on the disconnected phase of the line. The reflected waves at the far end of the line influence the arc current shape and its pulse width.

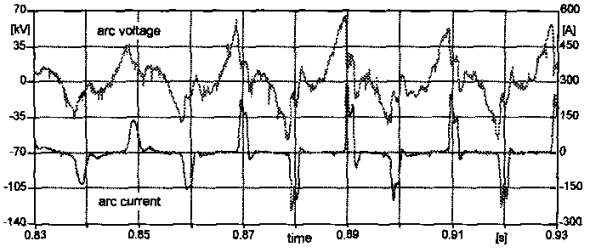

Fig. 8. Measured secondary arc voltage and current

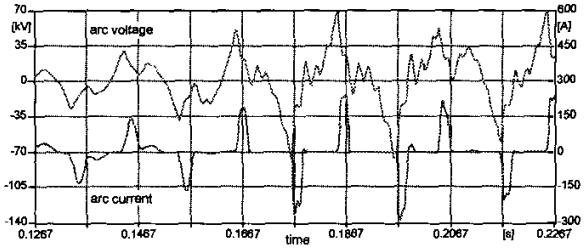

Fig. 9. Computed secondary arc voltage and current

The EMTP-ATP model of the test arrangement has been created using ATPDraw graphical preprocessor [7] and is shown in Fig. 7. Fig. 8 and 9 shows measured and computed secondary arc voltages and currents in a time interval where the arc is elongated suddenly and consequently the arc voltage and time constant changes rapidly, respectively.

In the simulation the arc time constant □is represented by the data (u'_0 and r'_0 remain unchanged) :

$$\tau_0 = 0.8 \text{ ms}, \quad \alpha = -1.6.$$

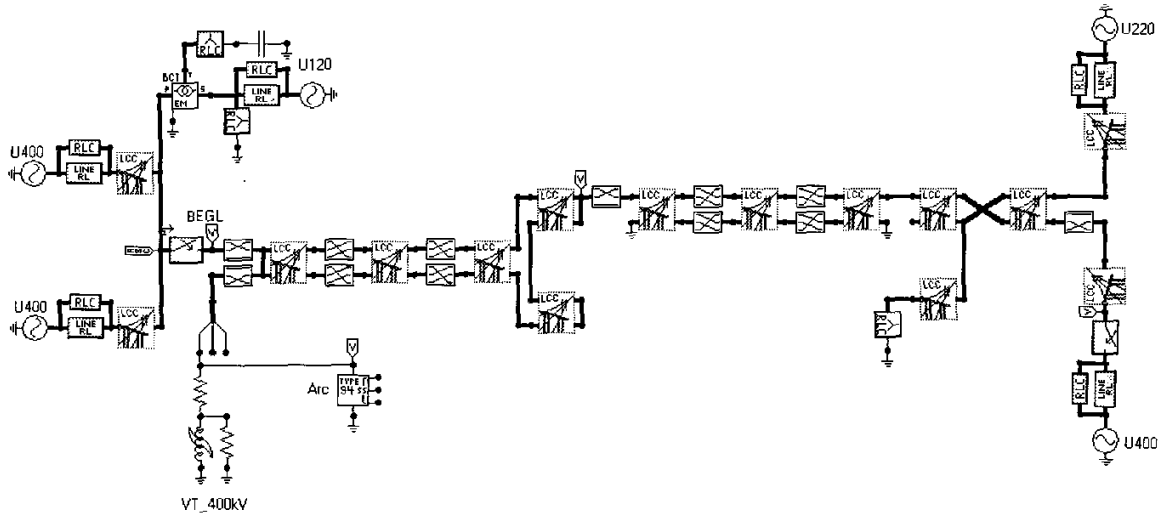

Fig. 7. ATPDraw circuit of the 400-kV system including the arc model

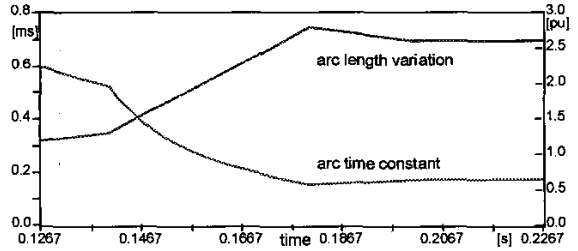

Fig. 10. Arc length and arc time constant variation in the simulation shown in Fig. 9

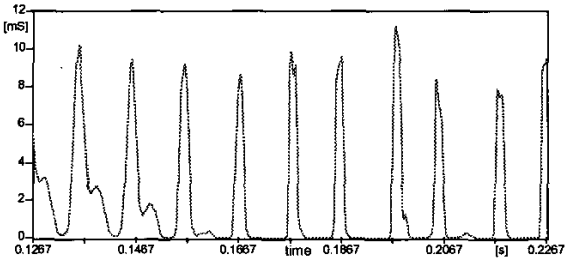

Fig. 11. Impulse-like varying arc conductance

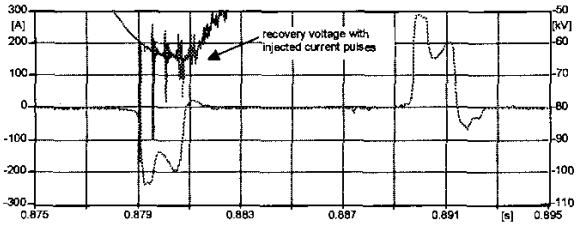

Fig. 12. Correlation between traveling waves and shape of the arc current

These current pulses initiate traveling waves on the line. The superposition of reflected waves produces a sudden current zero resulting in a increase of arc column resistance.

In order to show the correlation between traveling waves and the shape of arc current, an additional simulation has been performed by injecting a current pulse with a very small width (20 μs) into the line at the arc location by replacing the arc. Reflections take place at 1/3rd of the line and at open ends of the faulty phase. The simulation results with current pulse injection superposed on the recovery voltage and a cycle of measured arc current are shown in Fig. 12. The travel times obtained by the EMTP-ATP model of the line match practically with the changes in the waveform of the recorded arc current.

IV. Secondary Arc Interaction with a Shunt Compensated 750-kV Line

The influence of the line-side connected shunt reactors on the SPAR performance of the line was discussed in several papers in the past [8], [9], [10]. The secondary arc model presented in this paper is capable to reproduce the dynamic interaction of the arc with the shunt compensated line.

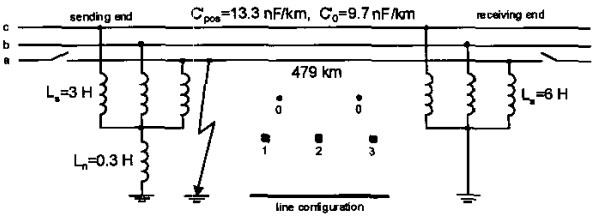

Fig. 13. An arc fault on a shunt compensated 750-kV line

A single-line-to-ground arc fault is simulated at sending end of a 479-km long, 750-kV single-circuit overhead line where four-legged shunt reactor (with a neutral coil) is installed on the line-side. The simplified diagram of the transmission line is shown in Fig. 13. The phase conductors consist of 4-bundle wires. The shunt reactor at the far end do not possess any neutral coil. Following data are used for the arc representation:

$$u'_0 = 0.9 \text{ kV/m}, \quad \tau_0 = 0.8 \text{ ms}$$
$$r'_0 = 40 \text{ m}\Omega\text{/m}; \quad \alpha = -0.5.$$

The initial arc length is assumed to be 15 m. A constant elongation speed for the arc is chosen such that the arc length will quadruple in 13 periods (0.26 s). The primary arc is initiated at t = 0.01 s. The pole of phase *a* of circuit-breakers at both line ends opens at t = 0.075 s. Fig. 14 shows the computed arc voltage and current waveforms. The shunt reactors produces a DC component in the initial part of the secondary arc current producing asymmetry in the current waveform of Fig. 14 around t = 0.2 s . The current of the corresponding leg of the shunt reactor at the sending end of the line is compared with the arc current in Fig. 15.

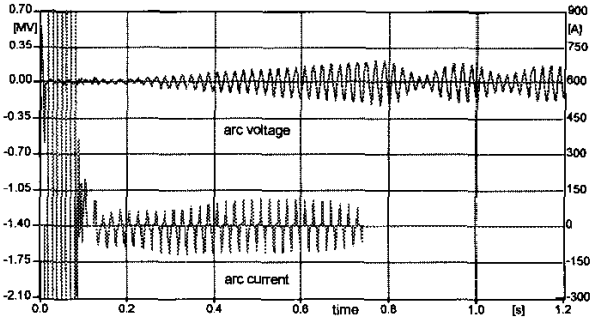

Fig. 14. Secondary arc voltage and current on the 750-kV line with four-legged shunt reactor

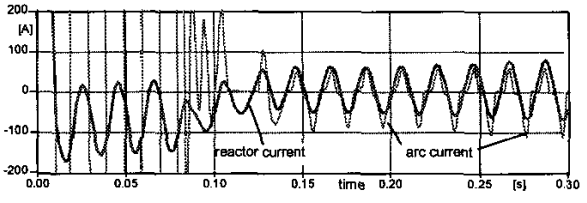

Fig. 15. Arc current and current of the shunt reactor (phase a) at the sending end of line

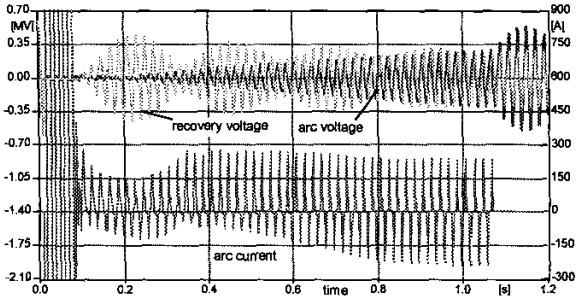

Fig. 16. Secondary arc voltage, arc current and recovery voltage on the shunt compensated line without neutral coil

Fourier analysis of the shunt reactor current (phase *a*) shown in Fig. 15 in the interval (0.25 s ... 0.27 s) results in

$$I_{DC} = 6.5 \text{ A};\ I_{50Hz} = 69.5 \text{ A (peak)}$$

After arc extinction at t = 0.75 s the recovery voltage in Fig. 14 shows low-frequency oscillations caused by the interaction of the shunt reactors with line capacitances.

It is known that the neutral coil aims to shorten the duration of the secondary arc by reducing the arc current and steepness of the recovery voltage at the fault location [8]. Shunt reactors without neutral coil has a negative impact on arc duration due to the relatively high oscillating recovery voltage. For comparison purpose a secondary arc simulation is performed using the same 750-kV transmission system, except the neutral coil at the sending end of the line is not taken into consideration. The computed arc voltage and current are shown in Fig. 16.

Additionally the recovery voltage is shown in this figure that is obtained by a separate computation, where the arc is replaced by a switch that opened at t = 0.1 s. Compared to the case with neutral coil (Fig. 15) the secondary arc current and recovery voltage are considerably higher causing a long secondary arc duration. With the same arc model following arc duration times are observed for both simulation cases:

- Shunt reactor with neutral coil : $t_{arc} = 0.67$ s (100 %)
- Shunt reactor without neutral coil : $t_{arc} = 1.0$ s (149 %)

The arc duration is expected to be 49 % longer, if the shunt reactor at sending end is not equipped with a neutral coil. The high amplitudes of the oscillating recovery voltage (Fig. 16) may prolong the arc duration due to likely re-ignition of the arc.

V. Conclusion

The arc model presented in this paper is capable to replicate the interaction of an arc fault through air with the remaining electrical network. Both arcing stages – primary and secondary arc – can be represented during single-phase autoreclosure as illustrated by simulation cases for an uncompensated 400-kV line and shunt compensated 750-kV overhead line.

The arc as a two-pole is modeled using type-94 component in the EMTP-ATP that enables simultaneous solution of the arc differential equation and electric circuit equations. MODELS, a general-purpose simulation language integrated in the EMTP-ATP, is used to describe the arc dynamics.

Due to highly random behavior of the secondary arc it is difficult to reproduce exact arc duration by digital simulations. In spite of this difficulty the arc model can be successfully utilized to find main factors influencing the secondary arcing process as illustrated in this paper by different simulation cases. The arc interaction with the electric circuit that the secondary arc may initiate traveling waves on the faulty phase due to impulse-like shape of the arc current can be shown also by digital simulations which are in agreement with the arc measurements. The interaction of the secondary arc with the line-side shunt reactors is shown for an existing 750-kV transmission line. The influence of a neutral coil on the secondary arc duration is illustrated by EMTP simulations.

VI. Acknowledgement

The activity reported in this paper has been partly supported by the Hungarian Research Fund under contract OTKA T-035178. Authors acknowledge the contribution of the Hungarian Power Companies Ltd. to the field measurements.

VII. References

[1] M. Kizilcay, K.-H. Koch, "Numerical fault arc simulation based on power arc tests", *ETEP Journal*, vol. 4, no. 3, pp. 177-186, May/June 1994.

[2] L. Prikler, M. Kizilcay, G. Bán, P. Handl, "Improved secondary arc models based on identification of arc parameters from staged fault test records", presented at the 14th Power System Computation Conf., Sevilla, Spain, June 2002.

[3] M. Kizilcay, T. Pniok, "Digital Simulation of Fault Arcs in Power Systems", *ETEP Journal*, vol., 1, no. 1, pp. 55-60, 1991.

[4] *Alternative Transient Program Rule Book*, Can/Am EMTP User Group, USA, 1997.

[5] H. J. Haubrich, et al., "Single-Phase Auto-Reclosing in EHV Systems" *CIGRE* 1974, Rep. 31-09.

[6] A.T. Johns, R.K. Aggarwal, Y.H. Song, "Improved Techniques for Modeling Fault Arcs on Faulted EHV Transmission System", *Proc. IEE – Generation, Transmission and Distribution*, vol. 141, no. 2, pp. 148-154, 1994.

[7] Prikler L, Høidalen HK. ATPDraw version 3.5 for Windows9x/NT/2000/XP-User's Manual. SINTEF Energy Research AS, Norway, TR F5680, ISBN 82-594-2344-8, Aug 2002.. http://www.eeug.org/files/secret/atpdraw

[8] G. Bán, L. Prikler, G. Banfai, "The Use of Neutral Reactors for Improving the Successfulness of 3-phase Reclosing", presented at the IEEE Budapest Power Tech'99 Conference, Budapest, Hungary, Aug 29 – Sept 2, 1999.

[9] IEEE Power System Relaying Committee Report, "Single phase tripping and auto reclosure of transmission lines", *IEEE Trans. Power Delivery*, vol. 7, no. 1, pp. 182-192, Jan. 1992.

[10] E. W. Kimbark, "Selective-pole switching of long double-circuit EHV lines", IEEE Trans. Power App. & Systems, vol. PAS-95, no. 1, pp. 219-230, Jan./Feb. 1976.

VIII. BIOGRAPHIES

Mustafa Kizilcay (M'94) was born in Bursa, Turkey in 1955. He received the B.Sc. degree from Middle East Technical University of Ankara in 1979, Dipl.-ing. degree and Ph.D. degree from University of Hanover, Germany in 1985 and 1991. From 1991 until 1994, he was as System Analyst with Lahmeyer International in Frankfurt, Germany. Currently, he is Full Professor for Power Systems at Fachhochschule Osnabruck, Germany. Dr. Kizilcay is winner of literature prize of Power Engineering Society of German Electroengineers Association (ETG-VDE) in 1994. He is a Member of IEEE, CIGRE, VDE and VDI in Germany.

Gábor Bán (M'87. F'94) was born in Kiskunhalas, Hungary in 1926. He received the M.Sc.degree from the Budapest University of Technology and Economics in 1950, PhD degree (1960) and DSc degree (1980) from the Hungarian Academy of Science (HAS). His employment experience included the Budapest Electric Company, the Electric Power Research Institute, Budapest. Since 1968 he has been a professor of the Budapest University of Technology and Economics. To Dr. Bán were awarded the Price of the HAS (1970), the Hungarian State Price (1980). He became the Eötvös Laureate of the HAS in 1997. He is a Fellow of IEEE and the Hungarian Academy of Engineers, a Distinguished Member of CIGRÉ and a member of the Hungarian Electrotechnical Association.

László Prikler (M'92) was born in Mosonmagyaróvár, Hungary on March 7, 1962. He received the M.Sc degree in Electrical Engineering from the Technical University of Budapest in 1986. Following graduation he joined the academic staff of the Department of Electric Power Systems of the same University. His main research interest is computer simulation of power system transients. In parallel with his academic carrier he is working for as consultant and managing director of his own enterprise Systran Engi. Services Ltd. Mr. Prikler is a Member of IEEE Power Engineering Society and the Hungarian Electrotechnical Association. Mr. Prikler was awarded by the Chapter Regional Outstanding Engineer Award by the Region 8 of IEEE in 2000. He was the publication committee chairman of Budapest PowerTech'99 and chairman of IPST'99.

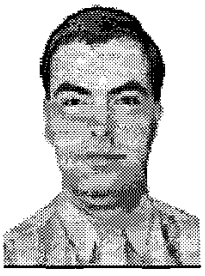

Péter Handl was born in Pécs, Hungary, on July 11, 1977. He studied at the Budapest University of Technology and Economics. After receiving the MSc degree in 2000 he is a postgraduate student at the Department of Electric Power Engineering. His main fields of interest are transients in the high voltage power systems, specially the transients caused by lightning flashes and the secondary arcs. He is a holder of a scholarship at the National Power Line Company in Hungary.